JOURNAL OF WATER AND LAND DEVELOPMENT
ISSN 1429–7426, e-ISSN 2083-4535

Polish Academy of Sciences (PAN), Committee on Agronomic Sciences
Section of Land Reclamation and Environmental Engineering in Agriculture
Institute of Technology and Life Sciences (ITP)

JOURNAL OF WATER AND LAND DEVELOPMENT
2020, No. 45 (IV–VI): 10–18
https://DOI.org/10.24425/jwld.2020.133041

Available (PDF): http://www.itp.edu.pl/wydawnictwo/journal; http://journals.pan.pl/jwld

Received 22.08.2019
Reviewed 19.12.2019
Accepted 03.01.2020

MgFe-doubled layers hydroxide intercalated with low cost local adsorbent using for removal of lead from aqueous solution

Hayder M. ABDUL-HAMEED[1)], Maad F. AL JUBOURY[2)] ✉

[1)] University of Baghdad, Faculty of Engineering, Baghdad, Iraq
[2)] Kerbala University, Faculty of Engineering, P.O. Box 1125, Freaha, Kerbala, Iraq and University of Baghdad, Faculty of Engineering, P.O. Box 17635, Jadiriya, Baghdad, Iraq

For citation: Abdul-Hameed H.M., Al Juboury M.F. 2020. MgFe-doubled layers hydroxide intercalated with low cost local adsorbent using for removal of lead from aqueous solution. Journal of Water and Land Development. No. 45 (IV–VI) p. 10–18. DOI: 10.24425/jwld.2020.133041.

Abstract

A new composite adsorbent was prepared by modifying low cost local adsorbent (LCL) using MgFe layered double hydroxide (LDH). This low cost local adsorbent was also prepared from the activation of date palm leaf derived from agricultural waste. In comparison to the low LCL, the adsorption capacity of the new composite adsorbent (LCL/MgFe-LDH) was improved. This was measured in terms of its ability to remove lead from wastewater. The Scanning electron microscope (SEM), Energy dispersive spectroscopy (EDS), Fourier-transform infrared spectroscopy (FTIR) and the specific surface area by the (Brunauer, Emmett and Teller) theory (BET) tests were conducted for the characterisation of LCL and LCL/MgFe-LDH. The behaviour of the lead adsorption processes by using LCL/MgFe-LDH as adsorbent was investigated in batch experiments by examining different values of solution pH, contact time, adsorbent dose and initial Pb^{2+} concentration. High removal efficiency was exhibited by LCL/MgFe-LDH, a value almost double that of LCL. This was attributed to the increase in surface area of LCL/MgFe-LDH (79.7 $m^2 \cdot g^{-1}$) in contrast to the surface area of LCL (24.5 $m^2 \cdot g^{-1}$). The Freundlich equations and pseudo-second-order kinetics model were appropriate for the provision of adsorption equilibrium data for Pb^{2+} on adsorbents. These results reveal the great potential of the new composite adsorbent (LCL/MgFe-LDH) if applied to the absorption of heavy metal ions.

Key words: *adsorption, agriculture waste, composite adsorbent, heavy metals, leaf date palm*

INTRODUCTION

Freshwater is the chief constituent of the planet and is essential for the survival of all living organisms [AZMERI, YULIANUR 2019; SHAFIQ *et al.* 2018]. Presence of heavy metals in the aquatic environment are being increasingly monitored as a result of growing urbanisation and industrialisation [HUR *et al*. 2015]. Heavy metals are the main pollutants of water (e.g. Cd, Zn, Ni, Cu and Pb). They accumulate in living tissue and are not biodegradable. As a result of this, both aquatic ecosystems and human health are under constant threat from these pollutants [KURNIAWAN *et al*. 2006; OMO-OKORO *et al*. 2018]. Wastewater resulting from different human activities such as industry, agriculture and urbanisation contains certain concentrations of various heavy metals. The removal of heavy metals from wastewater is essential to comply with environmental regulations and, of course, for the sake of human health and safety [MAHAGAMAGE, MANAGE 2018; SADON *et al*. 2014]. Lead is a metal of high toxicity. Exposure to lead toxicity has both chronic and acute effects on human health and the living environment. The existence of lead in the living environment is a cause for concern as lead does not degrade in nature and thus remains in circulation indefinitely [WANI *et al*. 2015].

Recently, layered double hydroxides (LDHs) have begun to be considered as an alternative adsorbent in treatment techniques [BARAKAT 2011; MOHAMMED, SAMAKA 2018]. LDHs are a class of two-dimensional nanostructured anionic clays. The lamellar structure of an LDH de-

pends on positively charged brucite-like layers similar to sheets with water molecules and anion-intercalated layers [LIANG *et al*. 2013].

In nature, layered double hydroxides can be present as minerals such as takovite (NiAl LDH), pyroaurite (MgFe LDH) and hydrotalcite (MgAl LDH). The anion interlayer is commonly a carbonate, however, sulphates and chlorides are often found as well. The formation of LDH is relatively simple in the laboratory [ROJAS 2016].

A higher anion exchange capacity combined with a large surface area and high surface activity make LDH an effective adsorbent of various anion pollutants [AYAWEI *et al*. 2015]. Furthermore, the cost efficiency, variable preparation, readily manipulated properties and versatility of LDH has led to an increased level of attention regarding the use of organo-LDH and LDH. Generally, LDHs are used in adsorption, ion exchange and catalysis [FAISAL, NAJI 2019]. In order to decontaminate polluted water, an adsorbent from organo-LDH and LDH can be applied to remove anions of toxic metals from an aqueous solution [TRAN *et al*. 2018].

Previous studies have demonstrated that organic anions (malate and citrate) coated with MgAl-LDH [TRAN *et al*. 2018], (CO_3)/CoMo-LDH [MOSTAFA *et al*. 2015] and MgFe-LDH, and loaded with magnetic (Fe_3O_4) carbon spheres [XIE *et al*. 2019], show higher attraction to lead than to natural LDH adsorbents.

Heavy metals present in wastewater and water are becoming an increasing public concern as a result of their impact on human health in regard to their carcinogenic and toxic nature. Thus, in drinking water, the concentration limit of lead is set at a maximum of 0.0015 $mg \cdot dm^{-3}$, as ruled by the World Health Organization [SIEGEL 2002].

Low-cost adsorbents made using natural date palm leaf (LCA) from agricultural waste are characterised by a low adsorption efficiency. The heavy metal adsorption capacity for LCA can be improved by processes such as thermal treatment, surface modification and activation [AHMED, THEYDAN 2012]. The adsorption capacity of obtained modified LCA is higher compared to pure LCA due to an increase in its surface area [KHADHRI *et al*. 2019]. However, the lead ion adsorption on the MgFe-LDH intercalated by low cost local adsorbent (LCL) (derived from activation of date palm leaf) has not yet been reported.

In this study, the process of modifying MgFe-layered double hydroxide with low cost local adsorbent (LCL) to create a new composite adsorbent (LCL/MgFe-LDH) was investigated. More specifically, the activation of date palm leaf derived from agricultural waste was explored in relation to its ability to create a low cost local adsorbent (LCL). The behaviour of the lead adsorption processes by using LCL/MgFe-LDH as adsorbent was investigated using the optimum value of different parameters. The removal of lead from aqueous solution was examined by using the new composite adsorbent.

STUDY METHODS

MATERIALS

The date palm leaf was obtained from southern Iraq as agricultural waste from local palm trees. Other chemicals (NaOH, HCl, $Mg(NO_3)_2 \cdot 6H_2O$, $FeCl_3 \cdot 6H_2O$ and Na_2CO_3) were all of analytical grade. A $Pb(NO_3)_2$ solution made by Limited Fine-Chem SD, Indian Company, with a 1000 $mg \cdot dm^{-3}$ concentration was prepared and kept at the temperature of the laboratory (25°C). The pH of the solution prepared was adjusted by using 0.1 mol of HCl or 0.1 mol of NaOH as needed. For any required concentration of lead, the solution stock was used.

LOW COST LOCAL ADSORBENT/MGFE-LDH PREPARTION

The dirty particles were washed from the LCA using distilled water. The substance was dried by the air stream, and then cut and crushed. The sieves, ranging from 0.595 to 1.19 mm mesh size, were used to sieve the substance. Finally, to produce low cost local adsorbent (LCL), the sieved material was physically activated at the furnace for 4 h at 350°C. During the first 2 h, nitrogen gas flowed at a rate of 500 $cm^3 \cdot min^{-1}$ into the furnace, and during the following 2 h, carbon dioxide flowed into the furnace at a rate of 500 $cm^3 \cdot min^{-1}$. Figure 1 shows the process of preparation the low cost local adsorbent.

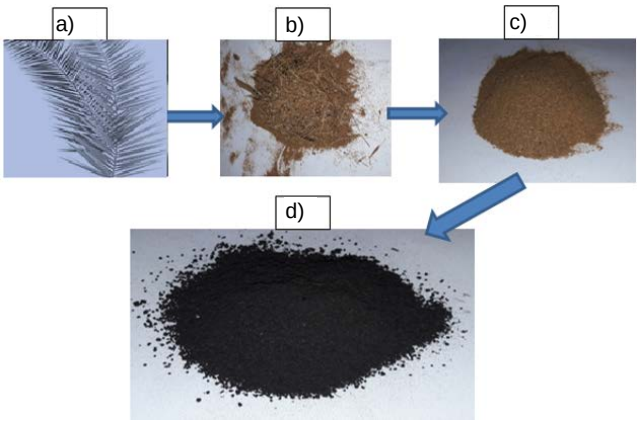

Fig. 1. Process of activated carbon preparation: a) natural date palm leaf, b) ground date palm leaf after grinding of natural date palm leaf, c) low cost adsorbent after sieving of ground date palm leaf, d) low cost local adsorbent after activation of low cost adsorbent; source: own elaboration

Layered double hydroxides (LDHs) were prepared using the co-precipitation method at the temperature of the laboratory. The solution containing $FeCl_3 \cdot 6H_2O$ and $Mg(NO_3)_2 \cdot 6H_2O$ using different molar ratios of (Mg:Fe) (1:1, 2:1, 3:1, and 4:1) was stirred at 200 ppm. Then, after obtaining the optimum adsorption capacity by using the optimum molar ratio, the subsequent experiment was conducted with different LCL dosages ranging from 0.05 to 2 g per 50 cm^3 of the solution to obtain the optimum dosage. Furthermore, a drop of NaOH (2 mol) and a drop of

Na_2CO_3 (0.2 mol) were added until a neutral pH of 7 was reached. This preparation took 1 h and following this, the solution was washed and filtered in deionised water. Finally, it was dried at 80°C for 24 h to obtain solids. The different Pb^{2+} adsorption capacity, obtained under diverse conditions of preparation, were compared to examine the effect of coating parameters.

ADSORPTION STUDIES

Batch experiments were carried out to determine the best parameters required for the most efficient adsorption. Furthermore, these experiments aimed to acquire equilibrium data of the treatment process. This data can then be used to study the adsorption mechanism and behaviour of the composite adsorbent. The parameters investigated included the adsorbent dosage [BENZAOUI *et al*. 2017], initial concentration of contaminants [BENZAOUI *et al*. 2017], pH of the solution [LAROUS *et al*. 2005] and contact time [SHARIFNIA *et al*. 2012].

Each flask from a series of 250 cm^3 conical flasks was filled with 50 cm^3 of an aqueous solution containing Pb^{2+}. The required pH of the solution prepared was adjusted and finally achieved by adding 0.1 mol HCl. To reach equilibrium, mixtures were shaken using a shaker and then filtered to obtain the adsorbent. The metal concentration, residual in the filtrate, was determined using an atomic absorption spectrophotometer flame (AAS). Kinetic studies of the solutions were examined through experiments replicated with varying parameters such as periods of time (5, 10, 20, 30, 60, and 180 min), pH (3, 4, 5, and 6), initial concentrations of contaminant (5, 10, 50, 100, 150, 200, 500 and 1000 $mg \cdot dm^{-3}$) and adsorbent dosages ranging from 0.02 to 0.5 g per 50 cm^3. Optimal results from these experiments at different values of each measured parameter were fixed so the optimum value of the four parameters used in the batch study were obtained.

According to the results from experimental work, the amount of contaminant held on the adsorbent was obtained using the equation below [WANG, CHEN 2009].

$$q_e = (C_o - C_e)\frac{V}{m} \quad (1)$$

Where: C_o, C_e represent the initial and equilibrium concentrations of contaminant in the solution ($mg \cdot dm^{-3}$), V is the volume of solution in the flask (dm^3) and m is the mass of adsorbent in the flask (g).

ADSORBENT CHARACTERIZATION

The chemical properties and molecular structure of LCA, LCL, LCL/MgFe-LDH and LCL/MgFe-LDH after lead adsorption were studied by Fourier transform infrared spectroscopy (FTIR), scanning electron microscope (SEM), energy dispersive spectroscopy (EDS) and specific surface area (BET). Using the FTIR spectrometer (Spectrum 100, PerkinElmer Corporation, America), the functional groups existed was measured. The images of the adsorbent produced by SEM showed the samples morphology, while the adsorbent chemical characterization was displayed using EDS. SEM and EDS images for the adsorbent were produced using Hitachi S-4800 SEM operating at 15 kV. The physical adsorption of gas molecules on a solid surface was explained by the theory of Brunauer–Emmett–Teller (BET), which can offer an analysis technique to measure the specific surface area of materials. The adsorption automated analyzer (Autosorb iQ – quantachrome instrument) was used for measuring the BET.

RESULTS AND DISCUSSION

CHARACTERIZATION OF THE SAMPLE

The FT-IR spectra of LCA, LCL, LCL/MgFe-LDH and LCL/MgFe-LDH after lead adsorption are shown in Figure 2. A broad peak observed at 3400 cm^{-1} refers to the stretching vibration of interlamellar water bonded to hydroxyl groups, water physically adsorbed (crystals outside water surface), and adjacent layers of the O-H groups [WANG *et al*. 2018]. The M-O and O-M-O lattice vibrations caused at 599 cm^{-1} exhibit a lower frequency peak (where M stands for metals) [JIA *et al*. 2019]. The MgFe--LDH modification of the LCL was successfully completed according to observation of new peaks at 1375 cm^{-1} in the

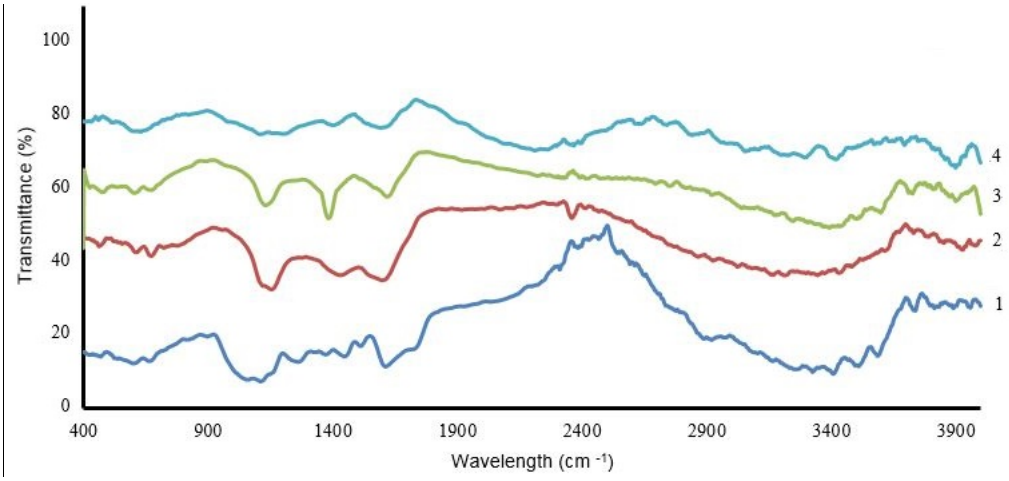

Fig. 2. Fourier-transform infrared spectroscopy (FTIR) of: 1) natural date palm leaf (LCA), 2) low cost local adsorbent (LCL), 3) LCL/MgFe-LDH, 4) LCL/MgFe-LDH after lead adsorption; source: own study

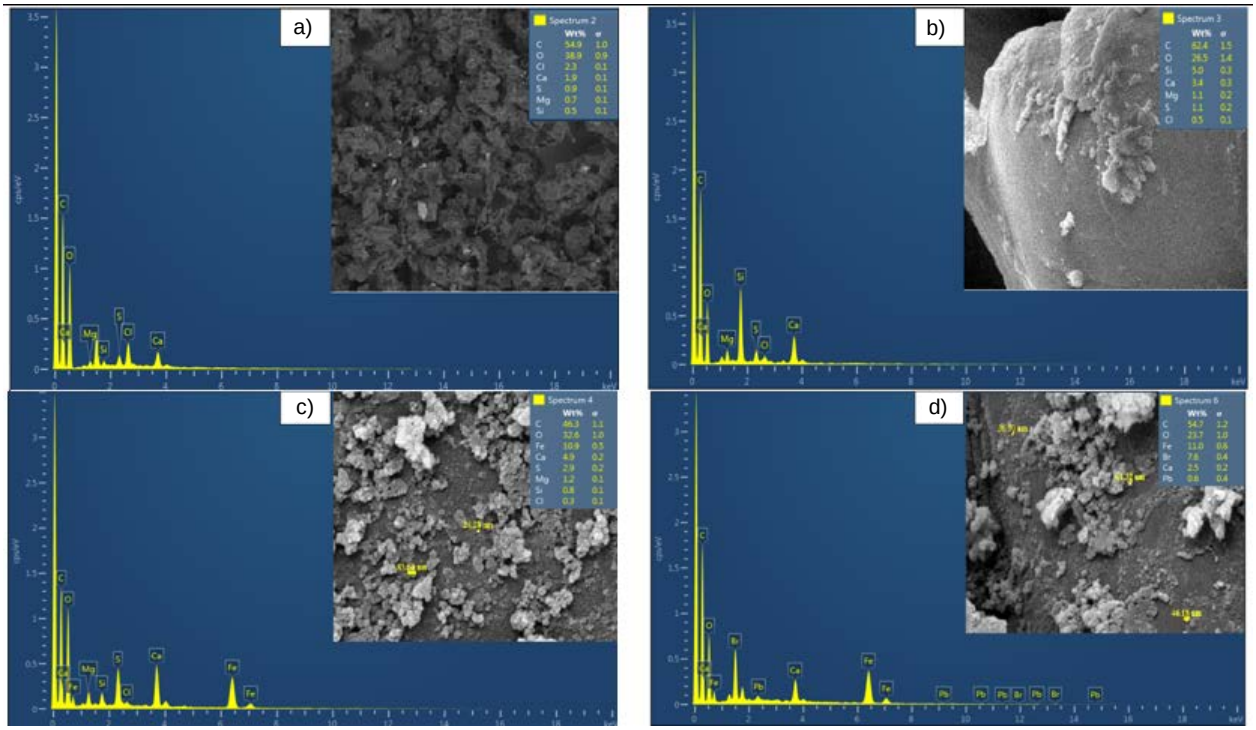

Fig. 3. Energy dispersive spectroscopy (EDS) and scanning electron microscope (SEM) images for the: a) natural date palm leaf (LCA), b) low cost local adsorbent (LCL), c) LCL/MgFe-LDH, d) after adsorption lead; source: own study

composites of LCL/MgFe-LDH compared to LCL, attributed to CO_3^{-2} band absorption asymmetric stretch [JIA *et al*. 2019]. After lead adsorption, it was observed that the vibrational modes amide I and amide II of proteins caused strong peaks at 1543 cm^{-1} (N-H deformation), and 1647 cm^{-1} (C=O stretching) respectively [MURDOCK, WETZEL 2009]. Thus, according to the sorbent FTIR, fewer functional group types appear on its surface.

The surface morphology of both LCA and LCL is shown in Figure 3. From this figure, it is evident that both have edges, sharp corners and rough surfaces, and their pore structure is compact and regular. The structure and large surface area of LCL allows it to function as the basis for other loading materials such as MgFe-LDH. The LCL/MgFe-LDH surface, which is produced by coating the LCL with MgFe-LDH, varies in size from 24.4–83.7 nm. The LDH has well-defined and regular particles and its structure is typically lamellar. Following the adsorption of lead, various regular hexagonal plates similar in structure to crystals (clearly shown in Fig. 3) bind with the surface of LCL/MgFe-LDH which has similar morphology to MgFe-LDH.

The EDS spectrum of LCL exhibits a high content of Ca, Si, Mg, O and C (Fig. 3). After modification, the content of Mg and Fe increase dramatically, providing evidence for the successful loading of MgFe-LDH on LCL using the co-precipitation method of synthesis. Following the adsorption of lead, a significant increase of its content on the sorbent suggests that the adsorption effect of the adsorbent on the contaminant is positive.

The BET, which refers to the theory by Brunauer Emmett Teller regarding the physical adsorption of gas molecules on a solid surface, is a technique to measure the specific surface area of materials [THOMMES *et al*. 2015]. Results of LCA, LCL, LCL/MgFe-LDH demonstrate that specific surface area increases from 0.8645 $m^2 \cdot g^{-1}$ for LCA to 24.5 $m^2 \cdot g^{-1}$ for LCL because of the activation process. This further increases to 79.6928 $m^2 \cdot g^{-1}$ for LCL/MgFe-LDH as a result of LDH loading. As previously mentioned, following MgFe-LDH loading to produce LCL/MgFe-LDH, adsorption capacity of the LCL is significantly increased.

EFFECT OF MG:FE MOLAR RATIO AND AMOUNT OF (LCL) COATED BY MG/FE-LDH

The effect of varying Mg:Fe molar ratios on lead adsorption was also investigated in this study. It cannot be ignored that the Mg:Fe molar ratio has a significant effect on adsorption capacities of LDH, as shown in Figure 4a. The highest adsorption capacity of LCL/MgFe-LDH for lead amounted to 11.1 $mg \cdot g^{-1}$ and were obtained with a three molar ratio of Mg:Fe, compared to LCL adsorption capacities for lead at a value of 6.1 $mg \cdot g^{-1}$. This leads to the conclusion that the Mg/Fe-LDH performance in the lead adsorption improved due to an increase in magnesium content. As the sorbent prepared with three Mg:Fe molar ratio featured the higher lead adsorption capacity, it was selected for the following experiments.

The amount of low cost local adsorbent (LCL) derived from the activation of date palm leaf used in a 50 cm^3 of solution varied from 0.05 to 2 g with a three Mg:Fe molar ratio (Fig. 4b. The lead adsorption capacity of the adsorbent rose according to the LCL dosage increase from 0.05 to 0.5 g. Thus, the 0.5 g dosage of LCL was proposed for coating.

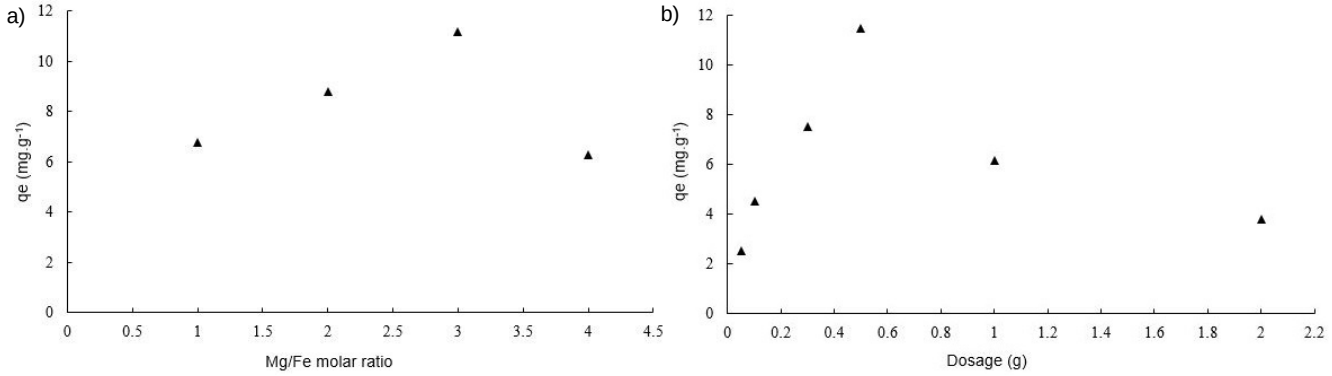

Fig. 4. Lead adsorption capacities by Mg/Fe-LDH under different conditions at (dosage = 0.04 g per 50 cm^3 of solution, pH = 5, adsorption time = 3 h): a) Mg/Fe molar ratios, b) low cost local adsorbent dosage; source: own study

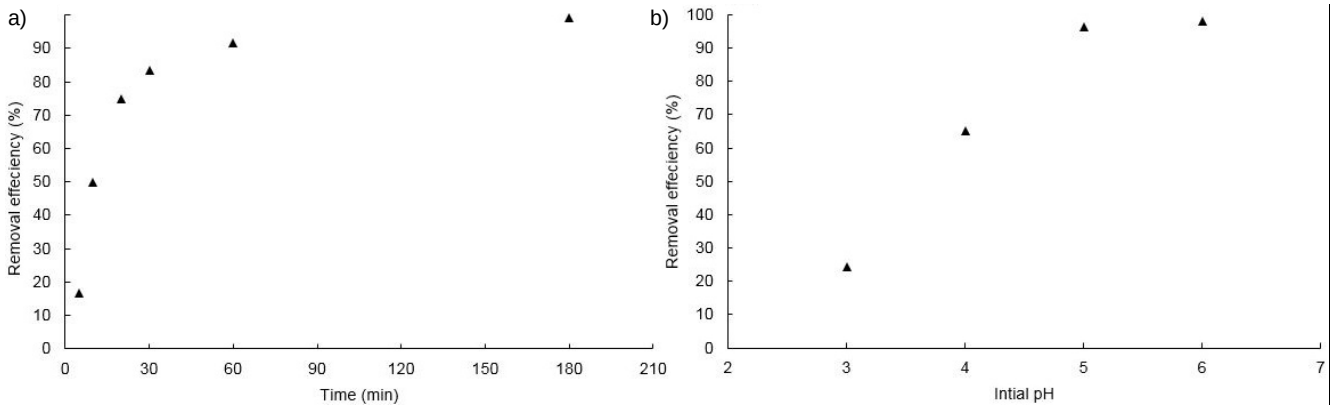

Fig. 5. Lead efficiency removal on the adsorbent at (agitation speed = 200 rpm; dose = 0.5 per 50 cm^3 of solution; T = 25±4°C) related to: a) contact time, b) initial pH; source: own study

EQUILIBRIUM TIME AND SOLUTION PH

In the batch experiments, the contact time should be fixed at a value when concentrations reach equilibrium. The lead removal was affected under contact time shown in Figure 5a. For the Pb^{2+} removal, 0.5 g from the reactive material was added to 50 cm^3 of the solution at room temperature. Typically, there are two stages of the metal sorption on the adsorbent. In the first stage, the adsorption is rapid, showing surface reaction, e.g. chemical (complexation on the surface) and physical (electrostatic sorption on the sorbent surface). The following stage includes a reaction that is metabolically active and slow. Figure 5a shows the limited percentage of Pb^{2+} according the contact time related to the metal solution and the adsorbent. The percentage of removed lead, as shown in Figure 5a, grows significantly according to the increased contact time. Initially, the adsorption was rapid, gradually slowing as time progressed. On the adsorbent surface, when the sorption sites decrease, sorption becomes slower. More than 99% of Pb^{2+} was removed in 1 h. In addition to this, at a contact time of greater than 1 h, the concentrations of metal remained steady. Residual metal concentrations did not change significantly at the time up to 2 h, yet, sorption experiments in other batches were conducted at this time.

The main parameter controlling the sorbent adsorption capacity is the solution pH. This is because of its influence on the pollutant's ionic forms and the sorbent surface properties [GARG *et al*. 2007]. The value of the pH has a significant effect on the sorption behaviour of the metal due to deprotonation and protonation of basic and acidic groups that influence the interaction of metal ions and the sorbent, the formation of metal hydroxides and the sorbent surface structure [ALKAN *et al*. 2008]. Figure 5b shows that the removal rate grew due to deprotonation and protonation of the sorbent basic and acidic groups. AL-HOMAIDAN *et al*. [2014] have reported a similar phenomenon whereby a gradual increase in solution pH causes a rise in metal sorption. On the cell surface, the polarity reactive sets were protonated in acidic conditions. More specifically, protons were occupied by the binding sites of the metal, causing a reduction in the metal sorption [ARECO *et al*. 2012].

THE INITIAL CONCENTRATION AND INITIAL DOSE EFFECT

Lead removal efficiency was examined experimentally at different initial concentrations of the metal. In these experiments, initial lead concentrations ranged from 10 to 1000 $mg \cdot dm^{-3}$ within 0.5 g of reactive material per 50 cm^3 of a solution. This solution was shaken at 200 rpm for 1 h and had an initial solution pH of 5. Figure 6a represents the lead removal efficiency for initial metal concentrations at

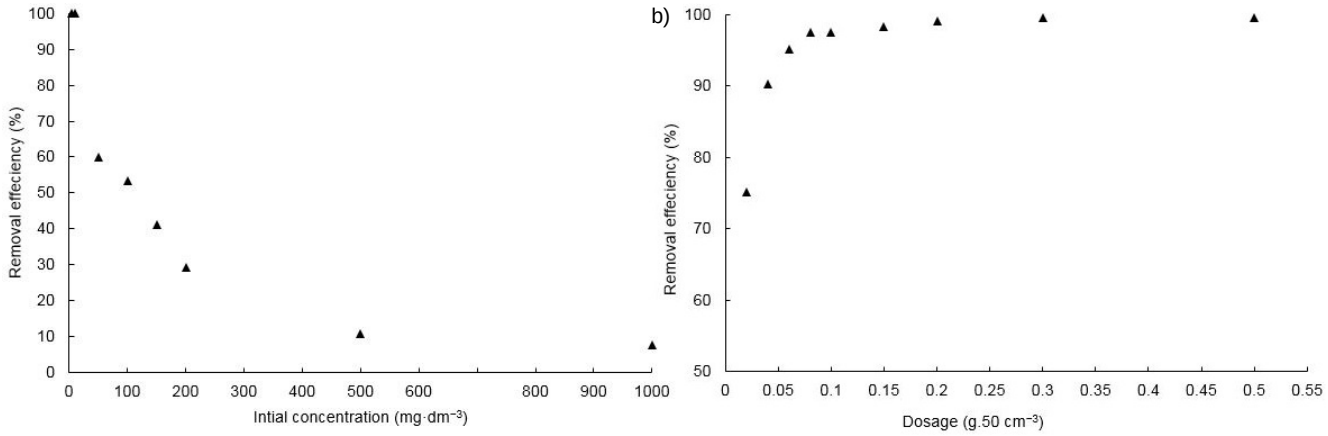

Fig. 6. Lead removal efficiency at (contact time = 1 h; agitation speed = 200 rpm; pH = 5; T = 25±4°C) effected by: a) initial concentration, b) the amounts of adsorbents dosage,; source: own study

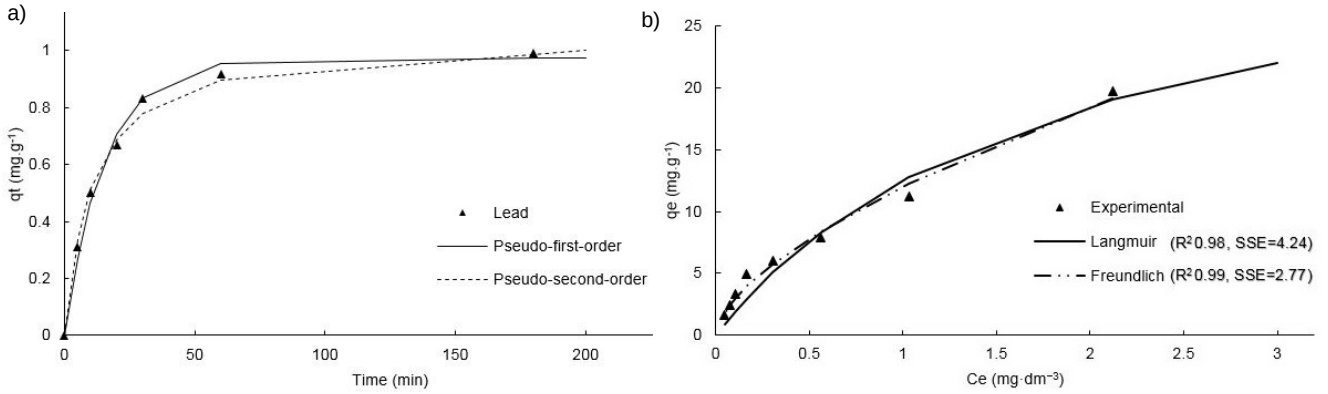

Fig. 7. Lead sorption at (200 rpm; 0.2 g per 50 cm^3; C_o = 5 mg·dm^{-3}; 25°C and pH =5): a) kinetics models calculated using nonlinear regression analysis, b) isotherm models on adsorbent; source: own study

equilibrium state. The results show that the metal removal was higher with the first values of initial concentrations. As the initial concentrations increase, the removal efficiency decreased. There was not a significant change in the amount of metal ions after 500 mg·dm^{-3}. This is resulting from the inability of metal ions to interact with the active sites of the reactive material. According to these results, as the concentration of metal in the solution increases, the sites become energetically less favourable [FAISAL, NAJI 2019].

In order to examine how the reactive material dosage affects the adsorption of lead, batch tests were conducted. Different amounts of the adsorbent were used, ranging from 0.02 to 0.5 g within a metal solution of 50 cm^3 at room temperature (25±4°C). Other parameters were kept as follows: contact time = 1 h; shaking speed = 200 rpm; pH = 5; C_o = 5 mg·dm^{-3}. Figure 6b shows the lead removal efficiency at differing amounts of the adsorbent. The lead removal efficiency grew as a result of the increased sorbent dosage ranging with the initial fixed metal concentration. The result described above was expected as it is established that an increase in sorbent dosage leads to a higher availability of active sites. The maximum rate of lead removal was reached with an adsorbent dosage of 0.2 g. With dosages higher than this, the amount of lead in the solution and its binding to the adsorbent remained fixed despite the increasing sorbent dosage.

ADSORPTION ISOTHERM AND KINETICS

The mechanism controlling lead adsorption on the adsorbent can be calculated as a chemical reaction according to the pseudo-first-order (Eq. 2) [HO 1999] and pseudo--second-order kinetics models (Eq. 3) [FAISAL, NAJI 2019]. These were both used to test the experimental data.

$$q_t = q_e(1 - \mathrm{e}^{-k_1 t}) \tag{2}$$

$$\frac{t}{q_t} = \left(\frac{1}{k_2 q_e^2} + \frac{t}{q_e}\right) \tag{3}$$

Where: q_t and q_e are the quantities of sorbate removed from the aqueous solution at time t, k_1 is the pseudo-first--order rate constant (cm^3·min^{-1}) and k_2 (g·(mg·min)$^{-1}$) represents rate constant of adsorption equilibrium in the second order reaction.

The nonlinear forms of kinetics adsorption models were examined by nonlinear regression analysis (Fig. 7a). The experimental and calculated values of the pseudo-second-order and pseudo-first-order for the Pb^{+2} sorption on the adsorbent are shown in Table 1.

If the pseudo-first-order kinetics model is applied, low value correlation coefficients are obtained. Calculated coefficients considered for the adsorption process were greater than 0.99 (Tab. 1) when the pseudo-second-order kinetics model was employed. A good concordance is shown

Table 1. Coefficients and sorption isotherm models for lead on adsorbent (200 rpm; 0.2 g per 50 cm^3; C_o = 5 $mg \cdot dm^{-3}$; 25°C and pH = 5)

Kind of model	Isotherm	Calculated parameters	Pb^{2+}
Isotherm models	Langmuir	q_m	26.24
		b	0.93
		R^2	0.98
		SSE	4.24
	Freundlich	K_F	11.36
		n	1.55
		R^2	0.99
		SSE	2.77
Kinetics models	pseudo-first-order	k_1	0.0647
		q_e	0.974
		R^2	0.9896
		SSE	0.006
	pseudo-second-order	k_2	0.0885
		q_e	1.056
		R^2	0.995
		SSE	0.0057
		q_e exp.	0.965

Explanations: q_m = maximum adsorption capacity, b = Langmuir constant, R^2 = coefficient of calculation, *SSE* = sum square error, K_F = Freundlich sorption coefficient, n = an empirical coefficient indicative of the intensity of adsorption, k_1 = pseudo-first-order rate constant, q_e = amount of solute adsorbed per unit weight of adsorbent at equilibrium and k_2 = pseudo-second-order rate constant.
Source: own study.

when the experimental and calculated adsorption capacities are compared. Thus, the lead adsorption process follows the pseudo-second-order kinetics model and as such, can be considered a chemisorption process.

The isotherms Langmuir and Freundlich model presented in Equation (4) [ALLEN *et al*. 2004] and Equation (5) [SAHA 2010] respectively, corresponded with the experimental data. Table 1 and Figure 7b show the results obtained for Pb^{2+} adsorption onto the adsorbent (coefficient of calculation (R^2), sum of squared errors (*SSE*) and isotherm parameters). The R^2 and *SSE* are used to select the best fitting model and the parameter. The R^2 represents the concordance degree between the experimental and predicted values by the suggested models. Ranging between 0 and 1, R^2 close to 1 confirms that the model has a high concordance between the actual and predicted values. The discrepancy of the data can be measured using *SSE*. A model has a good fit to the data when *SSE* is small [ABDULREDHA *et al*. 2018]. In this study, the R^2 and the *SSE* were compared for both models. The Freundlich model produced better prediction for the adsorption processes due to its lower *SSE* and higher R^2 comparing with the Langmuir isotherm model.

$$q_e = \frac{q_m b C_e}{1 + b C_e} \quad (4)$$

$$q_e = K_F C_e^{1/n} \quad (5)$$

Where: q_e = amount of solute adsorbed per unit weight of adsorbent at equilibrium ($mg \cdot g^{-1}$), C_e = equilibrium concentration of the solute in the bulk solution ($mg \cdot dm^{-3}$), q_m = maximum adsorption capacity, b = Langmuir constant related to the free energy of adsorption, K_F = Freundlich sorption coefficient ($(mg \cdot g^{-1}) \cdot (cm^3 \cdot mg^{-1})^{1/n}$), n = an empirical coefficient indicative of the intensity of adsorption.

After lead adsorption, the bands at 1375 cm^{-1} exhibited change which was as a result of an exchange of carbonate with lead. After biosorption, in general, groups of negatively charged peaks involved in the sorption process changed in intensity or moved (Fig. 2). Therefore, there are two mechanisms involved in the removal of the contaminate by the adsorbent. Metal ion exchange with carbonate is the first mechanism and leads to increased level of bicarbonate in the solution (Tab. 2). The second mechanism is the complexation of the metal with the functional group LCL.

Table 2. Carbonate and bicarbonate concentration after adsorption lead

Specification	Carbonate	Bicarbonate
	$mg \cdot dm^{-3}$	
The concentration at control	0.2	0.1
The concentration after adsorption lead	0.001	720

Source: own study.

CONCLUSIONS

A simple method was applied for loading Mg/Fe layered double hydroxides on low cost local adsorbents with a surface area of 79.6928 $m^2 \cdot g^{-1}$ according to the Scanning electron microscope (SEM), Energy dispersive spectroscopy (EDS) and Fourier-transform infrared spectroscopy (FTIR) characterisation. The activation of date palm leaf to produce low cost local adsorbent with a surface area of 24.5 $m^2 \cdot g^{-1}$ was successfully carried out. According to the characterisation of a new composite adsorbent and the increase in the surface area from 24.5 $m^2 \cdot g^{-1}$ to 79.6928 $m^2 \cdot g^{-1}$, the lead removal efficiency from aqueous solution was improved and the adsorption capacity was increased. The pseudo-second-order kinetics model was applied for adsorption batch experiments and the Freundlich model was used in the analysis of equilibrium data. The adsorption exhibited a chemisorption behaviour and occurred on heterogonous surfaces. LCL/MgFe–LDH demonstrated a relatively high adsorption capacity in the removal of lead amounted to 11.1 $mg \cdot g^{-1}$ when compared to natural LCL at a value of 6.1 $mg \cdot g^{-1}$. As a result, it can be considered the appropriate substance to remove lead from aqueous solutions.

REFERENCES

ABDULREDHA M., AL-KHADDAR R., JORDAN D., KOT P., ABDULRIHA A., HASHIM K. 2018. Estimating solid waste generation by hospitality industry during major festivals: A quantification model based on multiple regression. Waste Management. Vol. 77 p. 388–400. DOI 10.1016/j.wasman.2018.04.025.

AHMED M.J., THEYDAN S.K. 2012. Physical and chemical characteristics of activated carbon prepared by pyrolysis of chemically treated date stones and its ability to adsorb organics. Powder Technology. Vol. 229 p. 237–245. DOI 10.1016/j.powtec.2012.06.043.

AL-HOMAIDAN A.A., AL-HOURI H.J., AL-HAZZANI A.A. 2014. Biosorption of copper ions from aqueous solutions by *Spirulina platensis* biomass. Arabian Journal of Chemistry. Vol. 7. No. 1 p. 57–62. DOI 10.1016/j.arabjc.2013.05.022.

ALKAN M., KALAY B., DOGAN M., DEMIRBAS Ö. 2008. Removal of copper ions from aqueous solutions by kaolinite and batch design. Journal of Hazardous Materials. Vol. 153. No. 1–2 p. 867–876. DOI 10.1016/j.jhazmat.2007.09.047.

ALLEN S.J., MCKAY G., PORTER J. 2004. Adsorption isotherm models for basic dye adsorption by peat in single and binary component systems. Journal of Colloid and Interface Science. Vol. 280. No. 2 p. 322–333. DOI 10.1016/j.jcis.2004.08.078.

ARECO M.M., HANELA S., DURAN J., AFONSO M., SANTOS D. 2012. Biosorption of Cu(II), Zn(II), Cd(II) and Pb(II) by dead biomasses of green alga *Ulva lactuca* and the development of a sustainable matrix for adsorption implementation. Journal of Hazardous Materials. Vol. 213–214 p. 123–132. DOI 10.1016/j.jhazmat.2012.01.073.

AYAWEI N., EKUBO A.T., WANKASI D., DIKIO E.D. 2015. Synthesis and application of layered double hydroxide for the removal of copper in wastewater. International Journal of Chemistry. Vol. 7. No. 1 p. 122–132. DOI 10.5539/ijc. v7n1p122.

AZMERI A., YULIANUR A. 2019. Effects of irrigation performance on water balance: Krueng Baro Irrigation Scheme (Aceh – Indonesia) as a case study. Journal of Water and Land Development. No. 42 (VII–IX) p. 12–20. DOI 10.2478/jwld-2019-0040.

BARAKAT M. 2011. New trends in removing heavy metals from industrial wastewater. Arabian Journal of Chemistry. Vol. 4. No. 4 p. 361–377. DOI 10.1016/j.arabjc.2010.07.019.

BENZAOUI T., SELATNIA A., DJABALI D. 2017. Adsorption of copper (II) ions from aqueous solution using bottom ash of expired drugs incineration. Adsorption Science and Technology. Vol. 36 p. 114–129. DOI 10.1177/ 0263617416685099.

FAISAL A., NAJI L. 2019. Simulation of ammonia nitrogen removal from simulated wastewater by sorption onto waste foundry sand using artificial neural network. Association of Arab Universities Journal of Engineering Sciences. Vol. 26. No. 1 p. 28–34. DOI 10.33261/jaaru.2019.26.1.004.

GARG U.K., KAUR M.P., GARG V.K., SUD D. 2007. Removal of hexavalent chromium from aqueous solution by agricultural waste biomass. Journal of Hazardous Materials. Vol. 140. No. 1–2 p. 60–68. DOI 10.1016/j.jhazmat.2006.06.056.

HO Y.S., MCKAY G. 1999. Pseudo-second order model for sorption processes. Process Biochemistry. Vol. 34. No. 5 p. 451–465. DOI 10.1016/S0032-9592(98)00112-5.

HUR J., SHIN J., YOO J., SEW Y. 2015. Competitive adsorption of metals onto magnetic graphene oxide: Comparison with other carbonaceous adsorbents. The Scientific World Journal. Art. ID 836287. DOI 10.1155/2015/836287.

JIA Y., ZHANG Y., FU J. 2019. A novel magnetic biochar/MgFe-layered double hydroxides composite removing Pb^{2+} from aqueous solution: Isotherms, kinetics and thermodynamics. Colloids and Surfaces A: Physicochemical and Engineering Aspects. Vol. 567 p. 278–287. DOI 10.1016/j.colsurfa. 2019.01.064.

KHADHRI N., SAAD M., MOSBAH M., MOUSSAOUI Y. 2019. Batch and continuous column adsorption of indigo carmine onto activated carbon derived from date palm petiole. Journal of Environmental Chemical Engineering. Vol. 7. No. 1 p. 1–43. DOI 10.1016/j.jece.2018.11.020.

KURNIAWAN T., CHAN G., LO W., BABEL S. 2006. Physicochemical treatment techniques for wastewater laden with heavy metals. Chemical Engineering Journal. Vol. 118. No. 1–2 p. 83–98. DOI 10.1016/j.cej.2006.01.015.

LAROUS S., MENIAI A., LEHOCINE M. 2005. Experimental study of the removal of copper from aqueous solutions by adsorption using sawdust. Desalination. Vol. 185 p. 483–490. DOI 10.1016/j.desal.2005.03.090.

LIANG X., ZANG Y., XU Y., TAN X., HOU W., WANG L., SUN Y. 2013. Sorption of metal cations on layered double hydroxides. Colloids and Surfaces A: Physicochemical and Engineering Aspects. Vol. 433 p. 122–131. DOI 10.1016/ j.colsurfa.2013.05.006.

MAHAGAMAGE M., MANAGE P. 2018. Water quality and microbial contamination status of Madawachchiya, Padaviya and Kebithigollewa areas in Anuradhapura District, Sri Lanka. Journal of Water and Land Development. No. 42 p. 1–11. DOI 10.2478/jwld-2019-0039.

MOHAMMED A.A., SAMAKA I.S. 2018. Bentonite coated with magnetite Fe_3O_4 nanoparticles as a novel adsorbent for copper (II) ions removal from water/wastewater. Environmental Technology and Innovation. Vol. 10 p. 162–174. DOI 10.1016/j.eti.2018.02.005.

MOSTAFA M.S., BAKR A.S.A., EL NAGGAR A.M.A., SULTAN E.S.A. 2015. Water decontamination via the removal of Pb (II) using a new generation of highly energetic surface nanomaterial: $Co^{+2}Mo^{+6}$ LDH. Journal of Colloid and Interface Science. Vol. 461. p. 261–272. DOI 10.1016/j.jcis.2015. 08.060.

MURDOCK J.N., WETZEL D.L. 2009. FT-IR Microspectroscopy Enhances Biological and Ecological Analysis of Algae. Applied Spectroscopy Reviews. Vol. 44. No. 4 p. 335–361. DOI 10.1080/05704920902907440.

OMO-OKORO P.N., DASO A.P., OKONKWO J.O. 2018. A review of the application of agricultural wastes as precursor materials for the adsorption of per- and polyfluoroalkyl substances: A focus on current approaches and methodologies. Environmental Technology and Innovation. Vol. 9 p. 100–114. DOI 10.1016/j.eti.2017.11.005.

ROJAS R. 2016. Effect of particle size on copper removal by layered double hydroxides. Chemical Engineering Journal. Vol. 303 p. 331–337. DOI 10.1016/j.cej.2016.06.007.

SADON F., IBRAHEM A.S., ISMAIL K.N. 2014. Comparative study of single and multi-layered fixed bed columns for the removal of multi-metal element using rice husk adsorbents. Journal of Applied Sciences. Vol. 14. No. 12 p. 1234–1243. DOI 10.3923/jas.2014.1234.1243.

SAHA T.K. 2010. Adsorption of methyl orange onto chitosan from aqueous solution. Water Resource and Protection. Vol. 2. No. 10 p. 898–906. DOI 10.4236/jwarp.2010.210107.

SHAFIQ M., ALAZBA A., AMIN M.T. 2018. Removal of heavy metals from wastewater using date palm as a biosorbent: A comparative review. Sains Malaysiana. Vol. 47. No. 1 p. 35–49. DOI 10.17576/jsm-2018-4701-05.

SHARIFNIA S., KHADIVI M., SHOJAEIMEHR T., SHAVISI Y. 2012. Characterization, isotherm and kinetic studies for ammonium ion adsorption by light expanded clay aggregate (LECA). Journal of Saudi Chemical Society. Vol. 20 p. S342–S351. DOI 10.1016/j.jscs.2012.12.003.

SIEGEL F.R. 2002. Contaminant/natural background values. Timing and processes. In: Environmental geochemistry of potentially toxic metals. Berlin, Heidelberg. Springer p. 77–101.

THOMMES M., KANEKO K., NEIMARK A.V., OLIVIER J.P., RODRIGUEZ-REINOSO F., ROUQUEROL J., SING K. 2015. Physisorption of gases, with special reference to the evaluation of surface area and pore size distribution (IUPAC Technical Report). Pure and Applied Chemistry. Vol. 87. No. 9–10 p. 1–19. DOI 10.1515/pac-2014-1117.

TRAN H.N., LIN C.C., WOO S.H., CHAO H.P. 2018. Efficient removal of copper and lead by Mg/Al layered double hydroxides intercalated with organic acid anions: Adsorption kinet-

ics, isotherms, and thermodynamics. Applied Clay Science. Vol. 154 p. 17–27. DOI 10.1016/j.clay.2017.12.033.

WANG C., WANG H., GU G. 2018. Ultrasound-assisted xanthation of cellulose from lignocellulosic biomass optimized by response surface methodology for Pb(II) sorption. Carbohydrate Polymers. Vol. 182 p. 21–28. DOI 10.1016/j.carbpol.2017.11.004.

WANG J., CHEN C. 2009. Biosorbents for heavy metals removal and their future. Biotechnology Advances. Vol. 27. No. 2 p. 195–226. DOI 10.1016/j.biotechadv.2008.11.002.

WANI A.L., ARA A., USMANI J.A. 2015. Lead toxicity: A review. Interdisciplinary toxicology. Vol. 8. No. 2 p. 55–64. DOI 10.1515/intox-2015-0009.

XIE Y., YUAN X., WU Z., ZENG G., JIANG L., PENG X., LI H. 2019. Adsorption behavior and mechanism of Mg/Fe layered double hydroxide with Fe_3O_4-carbon spheres on the removal of Pb(II) and Cu(II). Journal of Colloid and Interface Science. Vol. 536 p. 440–455. DOI 10.1016/j.jcis.2018.10.066.